Recent motion of the African plates

C.J.H. Hartnady

Umvoto Africa (Pty) Ltd., P.O. Box 61, Muizenberg 7950, South Africa.
E-mail: chris@umvoto.com

Abstract

Models for the motion of the Nubia (NB) and Somalia (SM) plates, relative to the International Terrestrial Reference Frame (ITRF) and to each other, are derived from available public-domain data of the global tracking network for GPS satellites, processed at the Scripps Orbit and Permanent Array Center (SOPAC). The directional components of the station velocities are transformed into the geocentric XYZ reference frame of ITRF, and the plate angular-velocity (Euler) pole is obtained from the minimum eigenvector of the velocity orientation tensor. The angular rate is estimated from analysis of the residuals between measured and calculated velocities over an appropriate range of rotation rates. Three southern-hemisphere sites on the NB plate, specifically excluding the Hartebeesthoek (HRAO) site in South Africa, show <0.5 mm/yr motion relative to each other, their minimum mean residual velocity generally in the range 0.3-0.5 mm/yr. Relative to the stable NB plate interior, the HRAO site moves towards N129.5°E at 2.1 mm/yr, and the site at Richards Bay (RBAY) moves towards N151.2°E at 2.3 mm/yr, indicating that both lie on a separate Transgariep (TG) tectonic block. The new NB-SM Euler pole is nearly identical in loxcation to the pole for the last ~3 Myr, derived from geological data. However, the rate of rotation has increased by more than 70%, probably around 0.5 Myr ago in the Late Pleistocene. The SE-ward motions of RBAY and HRAO oppose the direction of slow NB-SM plate convergence in the area south of Mozambique. The faster convergent motion of the TG block relative to SM has implications for subduction initiation in this part of the Southwest Indian Ocean.

Introduction

The present-day velocities of the Earth's lithospheric plates provide kinematic boundary conditions important for many geological and geophysical studies, such as earthquake hazard assessment, research on seismogenic processes, and analyses of regional neotectonics. The global geological model NUVEL-1A [1,2] is based mainly on seafloor-spreading rates and directions measured at the mid-ocean ridges and uniformly standardised to date from the distinctive magnetic anomaly 2A (3.16 Ma or mid-Pliocene in age). NUVEL-1A was, however, unable to resolve the motions between the western (Nubian) and eastern (Somalian) parts of the African plate. Successful quantitative models of Nubia-Somalia (NB-SM) plate motion required more detailed regional assessments of data from the Red Sea [3,4] and the South West Indian Ridge [5,6].

Notwithstanding these recent successes in using the ~3-Myr average or "geological" velocity data to resolve NB-SM motion, there has long been a concern that NUVEL-1A or any other similar model may give biased or incorrect estimates of present-day motions for some plate pairs, because of post-Pliocene (<1.8 Ma) changes in the regional tectonic driving-force balance, leading to acceleration, deceleration, or changes in direction of some plates. With the development of modern space-geodetic techniques that measure plate motions on the time-scale of a few years to decades, [7,8] this concern (e.g, ref. 9) has proven real in the instance of the NB plate. Its space-geodetically-measured velocity - called "Recent motion" because it is probably representative over the Holocene or Recent epoch (last 10 000 years) [8] – is substantially different from the NUVEL-1A model for the whole or "composite" African plate.

Consequently the rate (but not direction) of NB-South America (SA) motion along the mid-ocean ridge in the South Atlantic Ocean has slowed appreciably at some time during the last 3 Myr (ref. 8, p.24-25). Apart from this NB-SA difference, there have also been changes in the rates and directions of relative plate motion along the Nubia-Arabia (AR) boundary (ref. 8, p.16 & Fig. 8) and along the complex NB-Eurasia (EU) boundary zone. [10]

Calais et al. [10] estimate NB-EU relative motion using a new set of GPS velocities from the NB and EU plates, and seafloor spreading rates and transform fault azimuths from the EU-North America (NA) and NB-NA plate boundaries. The latter improve significantly in quality and quantity on those used to derive NUVEL-1A. Simultaneous and separate inversion of the geodetic and geological data demonstrates that the two are mutually inconsistent at much greater than the 99% confidence level, which suggests that NB-EU plate motion has changed significantly since 3.16 Ma.

In order to test whether the NB-SM boundary [11] has undergone a comparable change between the late Pliocene and the present day, as previously suspected on geological and geophysical grounds, [9] I review the space-geodetic solutions [7,8] for the NB and SM plates, which are generally current to the year 2000, and update them using newer velocity estimates for key African stations in the continuously recording GPS network, current to epoch 2003.4151. The station velocity results (Table 1), which serve as input data to the revised modelling of NB and SM recent motions, are expressed in the current International Terrestrial Reference System (ITRS) of the International Earth Rotation Service (IERS).

Reference Frames

The quantitative analysis of the velocity field requires the definition of a reference frame for mapping velocities that is meaningful for tectonic interpretation. [12] In particular, velocities within an area of active deformation must be expressed in a regional reference frame that behaves more rigidly than the area under study. In the case of the better-covered EU plate, the accuracy of the NUVEL-1A plate model [2] is not sufficiently accurate to ensure an unbiased definition for rigid plates at the 2-3 mm/yr level [12]. The quantitative separation of motion between the African plates is only recently achieved in the NUVEL-1A context [5]. Moreover, the NB-SM Euler pole is located within the wide plate boundary, so that the relative velocity between the plates may locally be much less than 2 mm/yr, which makes the definition of a regional “stable reference frame” more problematic.

The year 2000 realization of ITRS (ITRF2000) is a global multi-technique geodetic solution [13-14] that provides accurate position and velocities at about 500 globally distributed control sites, and an accurate estimation of relative motions for 6 major tectonic plates. Five space-geodetic techniques contribute to the ITRF: Very Long Baseline Interferometry (VLBI), Lunar Laser Ranging (LLR), Satellite Laser Ranging (SLR), Global Positioning System (GPS), and Doppler Orbitography Radiopositioning Integrated by Satellite (DORIS). VLBI, LLR and SLR solutions in ITRF benefit from ~20 years of measurement. GPS and DORIS solutions include 2-10 years of continuous recording.

In global tectonics, the condition of “no net rotation” (NNR) of the entire rigid lithosphere is used to define an “absolute” reference frame [15], within which the geophysical model NNR-NUVEL-1A [2] describes the angular velocities of all plates. The ITRS also specifies a NNR condition, aligning the orientation-time evolution of the ITRF2000 by a consistent geodetic method that minimizes the global rotation rate between ITRF2000 and NNR-NUVEL-1A [16].

Methods

The present study is based on GPS data only for 8 African-region sites (Table 1 and Figure 1), provided through the Scripps Orbit and Permanent Array Center (SOPAC) in the University of California at San Diego. GPS site coordinates, ITRF2000 velocities, and time series are created at SOPAC by a "refined model" [17] that takes into account offsets (co-seismic or otherwise), linear velocity, and annual and semi-annual fluctuations (for stations that have at least two years and one year of data, respectively). The daily processed site positions calculated using the GAMIT and GLOBK software packages (http://www-gpsg.mit.edu/~simon/gtgk/) are data input to this model. SOPAC lists coordinates from the most recent weekly processing run, generated using data for that week only.

SOPAC also provides GPS position time series for stations (e.g., Fig. 2) for which all parameters are estimated with full white noise + flicker noise covariance based on a noise analysis. Parameter uncertainties are considered to be realistic estimates. For most stations a process of regional filtering is carried out in the space domain. By stacking the time series from a group of "core sites", a series containing common noises for the region is derived, which is then subtracted from individual time series to improve positional estimates.

The time-series for the station at the Hartebeesthoek Radio-astronomy Observatory (HRAO) in South Africa illustrates the derivation of the ITRF2000 velocity components in the North, East and Vertical directions (Fig. 2). In this study, the directional component (unit vector) of the resultant horizontal (N-E) station velocity (Table 1) is transformed into the geocentric XYZ reference frame of ITRF. In a graphical illustration (Fig. 3) of this procedure for the South African site at Sutherland (SUTH), the horizontal directional (large open square) lies in a geocentred plane (represented by the thin-dashed great circle in a lower or southern hemisphere stereographic projection) normal to the pole through the SUTH site (small solid square).

For two or more sites on a rigid plate of lithosphere, a plate angular-velocity (Euler) pole can be obtained graphically by constructing a great circle through the coordinate-transformed velocity vectors (solid great circles in top part of Figs. 3 and 4), and finding the pole normal to that plane (circled solid dots or target symbols in top part of Figs. 3 and 4). This technique is common in structural geology for defining the best-fitting cylindrical fold axis from poles normal to bedding planes, the "pi-circle method" [18]. In formal vector-statistical terms it is obtained numerically from the minimum eigenvector of the Scheidegger-Watson orientation tensor [19-20].

After prior solution for the Euler pole position by the above-mentioned numerical method, an angular rate of rotation is estimated from analysis of the residuals between measured and

calculated velocities over a small range of possible rotation rates (bottom sections of Figs. 3 and 4).

Results

The NB-ITRF200, SM-ITRF2000 absolute and the NB-SM relative angular velocities are tabulated (Table 2, boldface entries) along with other recent estimates of these plate-motion parameters [5,7-8], for purposes of comparison.

Nubia Angular Velocity

The site location data (smaller solid symbols) and antipodal locations of the geocentred site velocity vectors (larger open symbols) are shown for SUTH (square), N'Koltang, Gabon (NKLG, triangle) and Gough Island (GOUG, diamond) in a lower, southern hemisphere stereographic projection (Fig. 3 upper). In the ITRF frame these velocity directions are distributed along a ~40° arc of a well defined great circle (solid line), with the NKLG and GOUG directions at the data limits of this arc. The antipode (49.9°S 96.2°E) of the NB-ITRF2000 Euler pole (large target symbol) is the minimum eigenvector or axis of least moment of inertia of the velocity vector distribution.

The scalar rate of rotation is obtained by graphical analysis of the site residuals (open symbols) and mean residual (solid circles) over the range of values 0.253-0.262 mm/yr (Fig. 3 lower). The value preferred (0.258°/Myr), which is equal to that independently obtained by DeMets (pers. comm., 2002), is based on consideration of the least difference or deviation between site residuals and the mean, rather than on the minimum mean residual (0.29 mm/yr), which is obtained for a value of 0.256°/Myr (Fig. 3). This option gives more weight to the GOUG datum than to NKLG, which may be justified by the longer GPS time series for the former (Table 2).

Somalia Angular Velocity

The site location data (smaller solid symbols) and antipodal locations of the geocentred site velocity vectors (larger open symbols) are shown for Malindi, Kenya (MALI, square), and La Misere, Seychelles (SEY1, diamond) in a southern hemisphere stereogram (Fig. 4 upper). As only two directions are involved, the antipode (45.7°S 69.9°E) of the SM-ITRF2000 Euler pole (large target symbol) is in this case equivalent to a simple vector cross-product of the MALI and SEY1 unit vectors, which are separated by a ~20° angle of arc on the common great circle (solid line).

The scalar rate of rotation is obtained by graphical analysis of the site residuals (open symbols) and mean residual (solid circles) over the range of values 0.33-0.41 mm/yr (Fig. 4

lower). Likewise to the NB case, the value preferred (0.37°/Myr) is based on the least difference between site residuals and their mean, rather than on the minimum mean residual, which is obtained for a value of 0.35 mm/yr.

Nubia-Somalia Relative Motion

The NB-SM relative angular velocity, with an Euler pole close to 27°S 36°E (Table 2), is obtained by vector addition of the NB-ITRF2000 and ITRF2000-SM angular velocities.

Discussion

The velocity vector diagram is a useful tool for graphical representation of plate motions at a particular site, whether observed or modelled, relative or absolute. Its original and most frequent application in plate tectonics is in the analysis of velocity closure around, and the kinematic stability of, triple junctions between the major plates. [21]

Diagrams (Figs. 5-7) of the measured absolute-velocity vector, i.e., with ITRF2000 as the coordinate origin of the North velocity (Vn) and East velocity (Ve) axes, are presented for all of the sites listed in Table 1. In each of these diagrams, the thicker solid line from the origin (not shown in the enlargement) to the centre of the 1-σ error bars, is the GPS velocity measurement. Other solid or dashed lines, drawn from the (out-of-frame) origin to various symbols, represent model plate (NB or SM) velocities in ITRF2000. The direction and amount of the residual, i.e., the difference vector between model and observation, is easily seen and evaluated in these graphs.

Stable NB Reference Frame

The velocities of the four western sites (SUTH, NKLG, GOUG and MAS1 in Fig. 1) are used to constrain the present-day motion of NB (Fig. 3 and Fig. 5). In the previous GPS-based analysis, [8] the sites SUTH and GOUG were used to calculate the NB angular velocity, together with Maspalomas, Canary Isles (MAS*, composite of sites MAS1 and MASP linked by a published site tie) and also with HRAO and HAR* (Hartebeesthoek composite site). The NKLG site was not yet available, having only been commissioned during 2000, the year to which the earlier study was current. At this time, both SUTH and GOUG had records of about the same duration as NKLG has for this study (~3 years).

The NB angular-velocity model (Table 1) calculated from only SUTH, NKLG and GOUG (Fig. 3), provides a velocity fit that is within the 1-σ error limits of these three sites (Fig. 5). For both SUTH and NKLG, the new NB-ITRF2000 model shows a very slight counter-clockwise bias in direction (upper panels in Fig. 5), and for NKLG a slight overestimate in

speed (upper right in Fig. 5). For GOUG, the model's directional fit is close to perfect (lower left in Fig. 5), but the speed is underestimated.

The NB-ITRF97 angular-velocity model of Sella et al. [8] predicts velocity vectors for SUTH, NKLG and GOUG that are rotated a few degrees clockwise from the observed velocity, and lie outside the 1-σ error limits for Vn, especially in the case of GOUG (Fig. 5). It provides a fit to the data from MAS1 (lower right in Fig. 5) that is no better than the NB-ITRF2000 result, having a clockwise bias of about the same amount as the counter-clockwise bias of the latter. However, the Canary Isles are a neovolcanic massif of probable hotspot origins, extending into the Atlantic Ocean from the direction of the neotectonically active High Atlas and Anti Atlas mountains of Morocco. Some question may therefore arise as to whether MAS1 is really located on a stable part of the NB plate, or alternatively lies within the zone of influence of the EU-NB plate boundary.

A comparison of the MAS1 velocity with the model vectors derived from recent EU-ITRF96 and EU-ITRF97 angular-velocity models, respectively of Zhang et al. [22] and Sella et al.[8], shows that the EU-ITRF96 prediction fits the MAS1 data closely, whereas the improved EU-ITRF97 model is quite different.

The three sites used in the present NB-ITRF2000 solution are located around the continental margin of south-western Africa and an eastern South Atlantic core region of Early Cretaceous oceanic lithosphere within which little or no intraplate seismic activity is recorded (Fig. 1). Consequently their preferred status as a 3-site "A Priori Stable Nubia Reference Frame" or APSNuRF, following the EU plate precedent of an 8-site APSERF, [12] is tectonically appropriate.

Velocity of the SM plate

The present, minimal, 2-site solution for the angular velocity of the SM plate (Table 1) provides an exact directional fit to observed velocities (Fig. 6) at MALI and SEY1. However, MALI moves slower than the NB-ITRF2000 model prediction and SEY1 moves faster (solid square symbols in Fig. 6). In both cases the model solution lies outside the 1-σ error box on both Vn and Ve.

The REVEL model (SM-ITRF97; open square symbols) is also based on the data to year 2000 from only MALI and SEY1, except that the first year of data (1995-6) from SEY1 was omitted as being "particularly noisy" (ref. 8, p. 11-26). The REVEL model velocity for the longer MALI GPS time series is a closer fit than the new SM-ITRF2000 model (Table 1), although rotated some degrees clockwise from the data, being outside the 1-σ error for Vn

but within the 1-σ Ve error (Fig. 6 upper). However, it is a poorer fit to the 1995-2003 GPS time series for SEY1, being further outside the 1-σ error on Ve (Fig. 6 lower).

From this comparison it is evident that motion of the SM plate is still poorly constrained. Part of the problem may be that MALI is too close to the western boundary of the plate (Fig. 1), and is affected by localised tectonic deformation and build-up of elastic strain in the region of the triple junction between UN, RV and SM plates [11] around the Kilimanjaro-Chyulu Hills neovolcanic zone, or the Pangani Rift around the Kenya-Tanzania border area. If this is the case, then the SEY1 velocity, from a microcontinent centrally embedded within the oceanic lithosphere of the SM plate, may be a more reliable kinematic datum, and the 0.37°/Myr magnitude of SM-ITRF2000 angular velocity (Table 1) is an underestimate.

It is a matter of some concern that the GPS time series data for SEY1 is only current to epoch 2002.5767 (Table 2), because the improvement of the velocity determinations from this locality is essential for further progress. It is possible to augment the SM data set with velocity data measured by the DORIS technique at Reunion Island, but this has not been considered in the present study, which like the REVEL model [8] is restricted in its scope to GPS sites. Reunion is a very active hotspot volcano, and the velocity data from this site may be complicated by other localised geological factors, such as magma-chamber inflation or deflation, and/or large-scale mass movements of parts of the larger volcanic edifice. In this regard the extinct volcanic island of Mauritius, on an older portion of Reunion hotspot track, is a preferable future site for extending the continuously recording GPS network on the stable oceanic part of the SM plate.

Failing a future site in the north-eastern part of the Horn of Africa, e.g., Dante, Somalia or Socotra Island, South Yemen, which seems improbable for political reasons, a site at Fianarantsoa in Southern Madagascar, where an extension to the Global Seismographic Network is currently under construction, [23] would be useful. However, the level of seismic activity in and around Madagascar (Fig. 1) may signify that - like MALI - the Fianarantsoa site is possibly too close to the western boundary of the SM plate to be included in the definition of the stable SM reference frame.

Separation of Transgariep block motions

The 1996-2003 HRAO velocity datum (Table 1 and Fig. 2) is very close to 1986-1996 VLBI velocity result. [24] The significant difference between this VLBI result (Vn 16.64 mm/yr, Ve 17.41 mm/yr) and the NUVEL-1A African plate model for HRAO motion (Vn 20.08 mm/yr, Ve 20.68 mm/yr) indicated that HRAO lay within a deforming boundary zone between NB and SM, [9,11] and HRAO has therefore never formed part of the global set of ITRF stable

reference sites. In the REVEL model, however, the HRAO data is part of the defining set for NB angular velocity. [8]

Compared to the results of the present study (Fig. 7), the site velocities of HRAO and Richards Bay, South Africa (RBAY) are both more closely described by the REVEL model for the SM plate (open square circles on thin solid lines in Fig. 7). If the latter is preferred over the new SM-ITRF2000 model, then HRAO and RBAY must be considered to lie on the SM plate, even though the HRAO datum to year 2000 was integral to the definition of the REVEL NB-ITRF97 model.

In the new NB-ITRF2000 model, the HRAO site moves southeastward (N129.5°E) at 2.1 mm/yr, and the RBAY site moves in a more southward direction (N151.2°E) at 2.3 mm/yr. The magnitude of these difference vectors indicates that both sites definitely lie on a tectonic block kinematically separated from the NB plate. The western boundary of this Transgariep (TG) plate [11] is defined by a belt of seismicity and neotectonic faulting extending in an arc from the Zambia-Zimbabwe border in the Kariba Gorge area, through the Okavango Rift in northern Botswana, [25] the uplifted Khomas Hochland and Namaland Escarpment zones of Namibia, [26] and across South Africa and Lesotho around latitude 30°S (the "Senqu Seismic Belt"; cf. ref. 11, Figs. 2 and 3).

In the present-day plate boundary configuration of the southwestern Indian Ocean (Figs. 1 and 8), it is presently unclear whether the TG block shares a boundary with the SM plate. From the sparse seismic evidence it is instead possible that the Lwandle (LW) block, [11] consisting mainly of old (Late Jurassic-Early Cetaceous) oceanic lithosphere of the Mozambique Basin, [27] has recently decoupled from the SM plate. The LW-SM plate boundary could run through the weaker lithosphere of the island continent of Madagascar (Fig. 8), or along the reactivated Davie Fracture Zone (transform fault) [28] along the western continental margin of Madagascar.

If a separate LW block does not exist, then the RBAY site lies close to or within the TG-SM plate boundary (cf. Fig. 8). Relative to the SM-ITRF2000 model (solid square on thin solid line in Fig. 7), RBAY moves south-southeastward (N152.4°E) at 3.4 mm/yr, and HRAO moves in a similar direction (N160.4°E) at 3.7 mm/yr. In other words, the TG plate slowly *converges* (at ~3.5 mm/yr) on the SM plate in this area.

The velocity vector diagram (Fig.7) also shows that there would be even slower (1-2 mm/yr) convergence between NB and SM in this area, if either of these plates extended across this part of the TG domain. At HRAO the SM plate (solid square) moves north-northeastward relative to NB (solid circle), and at RBAY it moves northwestwards.

Implications for NB-SM geodynamics

This slow convergent motion of the two larger African plates is a consequence of the NB-SM Euler pole location near 27°S, 36°E (Table 2), close to the southern Mozambique coastline (Fig. 8). The new NB-SM Euler pole is nearly identical in position to the pole for the last ~3 Myr, derived from geological data.[5] However, the rate of rotation, which for the last 3 Myr averaged only 0.089°/Myr, has apparently increased by more than 70% to 0.148°/Myr (Table 2). This acceleration of NB-SM relative angular velocity probably occurred around 0.5 Myr ago in the Late Pleistocene. Evidence for the timing of this new phase of African neotectonics is found along the western boundary of the SM plate, from locations as far apart as the continental Kenya Rift, between the SM and UN plates, and the deep oceanic Natal Valley, along the southern part of the NB-SM (or NB-LW) plate boundary.

Volcano construction within the Kenya Rift began at less than 2 Ma, mostly younger than ~1 Ma. The inner rift valley experienced focused subsidence and intense faulting before and during the building of the large axial volcanoes. Starting in the Late Pleistocene, and particularly after about 100 ka, the inner rift entered a distinctly different phase of its volcanic history, with the catastrophic collapse of many of the axial volcanoes, producing large calderas. [29] The onset of the Recent phase of volcano-tectonic activity in the Kenya Rift area is related to a "best documented stress field change" [30] that occurred synchronously between the Tanzanian-Kenyan rifts along the NB-UN plate boundary and the northern Red Sea-Gulf of Suez area along the NB-AR plate boundary (Fig. 1). This Late Pleistocene rotation of the stress filed is dated to <600 ka (0.6 Ma) but >125 ka. [30]

In a 36 m-long core retrieved from the ocean floor of the Natal Valley, a history of largely hemipelagic sedimentation is revealed back to marine oxygen isotope stage 18 (~700 ka). [31] Around 400-500 ka, corresponding to a depth of at a depth of this record shows the beginnings of an episodic influx of thicker, coarse-sandy turbidite layers from a terrigenous clastic provenance, Seismic reflection evidence for massive recent slumping of the continental slope along nearby parts of the Agulhas Fracture Zone, [32] reinforces an interpretation of the Natal Valley turbidites as "seismite" deposits, following major prehistoric earthquakes along this section of the NB-SM (or NB-LW) plate boundary zone, analogous to the historic turbidite observed after the 1927 Grand Banks earthquake off the coast of eastern Canada.

This evidence from the south-eastern side of the Transgariep (TG) plate may be checked against the inland sedimentary record of the nascent Okavango Rift on its north-western side, of which at present only the maximum cumulative thickness of 200-300 m [25] is known.

Assuming that NB-TG relative motion of ~2 mm/yr applies across the full width of the rigid TG block and is concentrated along the main faults in Botswana, and that relative vertical motion along these Okavango border faults is roughly equal to the relative horizontal motion, then the onset of faulting and sediment accumulation in the Okavango is approximately dated to 400-600 ka.

The SSE-ward motions of RBAY and HRAO, producing the observed extensional tectonics along the Okavango Rift segment of the NB-TG boundary, are paradoxical in the context of slow NB-SM plate convergence in the area south of Mozambique. Somehow the TG block is escaping southeastwards at a faster rate than the southwestern portion of the SM plate (or the separate LW plate) is converging on NB in a northwards direction. The resolution of this paradox has implications for subduction initiation in this part of the Southwest Indian Ocean. [33]

One manner in which the TG, and possibly also the RV plate may be freed kinematically to move southwards against an opposing convergence of the SM and/or LW plates, is the commencement of "rollback"' along an incipient trench that has developed in the oldest oceanic crust along the north-western margin of the deep Mozambique Basin. [33] Rollback arises when subducted lithosphere sinks vertically into the asthenosphere at a faster rate than the horizontal velocity of the oceanic plate to which it remains attached.

Another possible mechanism for freeing the TG plate, is the faster "tectonic escape" of the adjacent LW block from the zone of NB-SM convergence. This lateral tectonic escape may be driven by the vice-like push and shear forces generated along a southwards-widening configuration of NB-LW and SM-LW boundaries in the northern Mozambique Basin, analogous to the faster westward tectonic escape of the Anatolian plate within the slower convergence zone between the Arabian and Eurasian plates. Alternatively or additionally, it may be driven by pull forces along a new subduction zone now developing farther south along the north-facing flanks of the Southwest Indian Ridge. There is some evidence for a ridge-parallel belt of "intraplate" earthquakes within the oceanic crust of this zone.

In the last-mentioned plate-tectonic scenario, the portion of the SWIR between ~30°E and ~50°E would evolve into a back-arc spreading centre bounding a system of island-arc microplate and trench (the name "Protea Plate" is suggested for this putative developing feature) that migrates northwards to consume the oceanic lithosphere adjacent to southwestern Africa and Madagascar.

Conclusions

Six main conclusions are drawn from the present study:

1. A tectonically stable core region of the NB plate is defined around a triangle of southern hemisphere GPS sites, with vertices at SUTH, NKLG and GOUG, covering the south-western part of the African continent and the eastern side of the South Atlantic Ocean, within which NB plate rigidity is tightly bound below an upper limit of ~0.4 mm/yr;
2. The NB-ITRF2000 Euler pole position defined on these three sites corresponds closely to other recent estimates, and the angular-velocity rate is within 0.005°/Myr of the REVEL angular-velocity model for NB motion;
3. The SM-ITRF2000 Euler pole, uniquely defined by velocity directionals (unit vectors) from only two sites (MALI and SEY1), differs substantially from other recent estimates, and the poorly constrained angular-velocity rate is greatly increased over previous estimates; i.e., 0.37°/Myr versus 0.31°/Myr for the REVEL model of SM plate motion;
4. The velocities of GPS sites HRAO and RBAY in the north-eastern part of South Africa, diverge in a south-easterly direction by 2.1-2.3 mm/yr from a reference frame attached to the rigid core of the NB plate. Because these sites are separated from stable NB by the neotectonically active arc between the Okavango Rift in Botswana and the Senqu Seismic Belt in South Africa and Lesotho, they are considered to lie on a separate Transgariep (TG) tectonic block, or microplate;
5. The new Euler pole of NB-SM relative motion coincides closely with the position near the Mozambique coastline, representative of NB-SM rotation over the past ~3 Myr, as defined by geologically-based (seafloor-spreading rate and fracture-zone trend) data from NB and SM boundaries with other plates along the Southwest Indian Ridge, in the Gulf of Aden and the Red Sea;
6. The greatly increased rate of NB-SM relative rotation dates from ~0.5 Ma, based on a probable correlation with distinct Late Pleistocene changes in crustal-stress regime, volcanic history and tectonic evolution along the western boundary of the SM plate, in places as widely separated as the Kenya Rift and the submarine Natal Valley offshore of South Africa.

Acknowledgements. This research was supported by Umvoto Africa (Pty) Ltd as part of its African GeoRisk Provention Strategy, and would not have been possible without the scientific efforts in the global “public good” of UCSD’s SOPAC.

References

1. DeMets C., Gordon R.G., Argus D.F. and Stein S. (1990). Current plate motions. Geophys. J. Int. 101, 425-478.
2. DeMets C., Gordon R.G., Argus D.F. and Stein S. (1994). Effect of recent revisions to the geomagnetic time scale on estimates of current plate motion. Geophys. Res. Lett. 21, 2191-2194.
3. Jestin F., Huchon P. and Gaulier J.M. (1994). The Somalia plate and the East African Rift System: present-day kinematics. Geophys. J. Int. 116, 637-654.
4. Chu D. and Gordon R.G. (1998). Current plate motions across the Red Sea. Geophys. J. Int. 135, 313-328.
5. Chu D. and Gordon R.G. (1999). Evidence for motion between Nubia and Somalia along the Southwest Indian Ridge. Nature 398, 64-67.
6. Lemaux J., II, Gordon R.G. and Royer J.-Y. (2002). Location of the Nubia-Somalia boundary along the Southwest Indian Ridge. Geology 30, 339-342.
7. Kreemer C. and Holt W.E. (2001). A no-net-rotation model of present-day surface motions. Geophys. Res. Lett. 28, 4407-4410.
8. Sella G. F., Dixon T. H. and Mao A., (2002). REVEL: A model for recent plate velocities from space geodesy. J. Geophys. Res. 107, 10.1029/2000JB000033, 1-30.
9. Ben-Avraham Z., Hartnady C.J.H. and le Roex A.P. (1995). Neotectonic activity on continental fragments in the Southwest Indian Ocean: Agulhas Plateau and Mozambique Ridge. J. geophys. Res. 100, 6199-6211.
10. Calais E., DeMets C. and Nocquet J.M. (2003) Evidence for a post-3.16 Ma change in Nubia-Eurasia plate motion, Earth and Planetary Science Letters, submitted (abstract online and published in Eos for American Geophysical Union, Fall meeting, San Francisco, 2002).
11. Hartnady C.J.H. (2002). Earthquake hazard in Africa: perspectives on the Nubia-Somalia boundary. S. Afr. J. Sci. 98, 425-428.
12. Nocquet J.M., Calais E., Altamimi Z., Sillard P. and Boucher C. (2001). Intraplate deformation in Western Europe deduced from an analysis of the ITRF97 velocity field, J. Geophys. Res. 106, 11239-11257.
13. Altamimi Z., Boucher C. and Sillard P. (2002). New Trends for the Realization of the International Terrestrial Reference System. Adv. Space Res. 30 (2), 175-184.
14. Altamimi Z., Sillard P. and Boucher C. (2002). ITRF2000 : A New Release of the International Terrestrial Reference Frame for Earth Science Applications. J. Geophys. Res. 107(B10), 2214, doi:10.1029/2001JB000561.
15. Argus D.F and Gordon R.G. (1991). No-net-rotation model of current plate velocities incorporating plate motion model NUVEL-1. Geophys. Res. Lett., 18, 2039-2042.

16. Altamimi Z., Sillard P. and Boucher C. (2003). The Impact of a No-Net-Rotation Condition on ITRF2000. Geophys. Res. Lett. 30(2), doi:10.1029/2002GL016279.
17. Nikolaidis R. (2002). Observation of Geodetic and Seismic Deformation with the Global Positioning System, Ph.D. Thesis, University of California, San Diego, ??? pp..
18. Ramsay J.G. (1967). Folding and Fracturing of Rocks. McGraw-Hill, New York, 568 pp.
19. Scheidegger A.E. (1965). On the statistics of the orientation of bedding planes, grain axes, and similar sedimentological data. U.S. Geol. Survey Prof. Paper 525-C, 164-167.
20. Watson G.S. (1965). Equatorial distributions on a sphere. Biometrika 52, 193-203.
21. McKenzie D.P. and Morgan W.J. (1969). Evolution of triple junctions. Nature 224, 125-133.
22. Zhang Z., Zhu W. and Xiong Y. (1999) Global plate motion models incorporating the velocity field of ITRF96. Geophys. Res. Lett.26, 2813-2816.
23. Incorporated Research Institutions for Seismology (2003). Global Seismographic Network station list (Online at web-site http://iris.synapse.ru/GSN/GSNstations.htm)
24. Ma C. and Ryan J. W. (1998). NASA Space Geodesy Program -- GSFC DATA Analysis -- 1998, VLBI Geodetic Results 1979-1998, NASA Report, August, 1998. (see http://www.hartrao.ac.za/geodesy/vlbi.gif).
25. Modisi M.P., Atekwana E.A., Kampunzu A.B. and Ngwisanyi T.H. (2000). Rift kinematics during the incipient stages of continental extension: evidence from the nascent Okavango rift basin, northwest Botswana. Geology 28, 939-942.
26. Korn H. and Martin H.M. (1952). The seismicity of South West Africa. Trans. Geol. Soc. S. Afr. 55, 85-88.
27. Martin A.K. and Hartnady C.J.H. (1986). Plate tectonic development of the southwest Indian Ocean: a revised reconstruction of east Antarctica and Africa. J. Geophys. Res. 91, 4767-4786.
28. Raillard S. (1990). Les marges de l'Afrique de l'Est et les zones de fracture associées: Chaîne Davie et Ride du Mozambique - Campagne MD-60/MACAMO-II, Thesis, Université Pierre et Marie Curie, Paris, 272 pp.
29. Bosworth W., Burke K. and Strecker M. (2000). Magma chamber elongation as an indicator of intraplate stress field orientation: "borehole break-out mechanism" and examples from the Late Pleistocene to Recent Kenya Rift Valley. In: Stress, Strain and Structure, A volume in honour of W D. Means. Eds: M.W. Jessell and J.L.Urai. Volume 2, Journal of the Virtual Explorer. http://www.virtualexplorer.com.au/VEjournal/2000Volumes/Volume2/www/contribs/bosworth/index.html)
30. Bosworth W. and Strecker M.R. (1997). Stress field changes in the Afro-Arabian rift system during the Miocene to Recent Period. Tectonophysics 278, 47-62.

31. Chen M-T., Bertrand P., Balut Y., Schneider R., Rogers J. and Taiwan IMAGES participants (1998). IMAGES II cruise (NAUSICAA) explores Quaternary climatic variability and linkage of Benguela and Agulhas Current Systems in the Southern Indian-Atlantic ocean: Participation by consortium of Taiwan institutions (coordinated by National Taiwan University). J. Geol. Soc. China 41: 73-80.
32. Niemi T. M., Ben-Avraham Z., Hartnady C.J.H. and Reznikov M. (2000). Post-Eocene seismic stratigraphy of the deep ocean basin adjacent to the southeast African continental margin: A record geostrophic bottom-current systems, Marine Geology 162, 237-258.
33. Hartnady C.J.H. (1990). Seismicity and plate boundary evolution in southeastern Africa. S. Afr. J. Geol. 93, 473-484.
34. Triep E.G. and Sykes L.R. (1997). Frequency of occurrence of moderate to great earthquakes in intracontinental regions. J. geophys. Res. 102, 9923-9948.
35. SOPAC .. http://sopac.ucsd.edu/cgi-bin/refinedTimeseriesListing.cgi

TABLES

Table 1. Site Positions and Velocities relative to ITRF2000

Site	Position		Velocity						Time series	
	°N	°E	North		East		Vertical		Start	End
Nubia plate										
MAS1	27.764	-15.633	16.43 ±	0.26	16.13 ±	0.47	1.80 ±	1.16	1994.4260	2003.4151
NKLG	0.354	9.672	18.12 ±	0.67	21.79 ±	1.45	-2.12 ±	2.19	2000.2500	2003.4151
SUTH	-32.380	20.810	17.61 ±	0.65	15.92 ±	0.86	2.90 ±	1.30	1998.2890	2003.4151
GOUG	-40.349	-9.881	18.03 ±	0.62	20.26 ±	1.17	-10.79 ±	1.95	1998.6205	2003.4151
Somalia plate										
MALI	-2.996	40.194	13.51 ±	0.45	26.41 ±	1.16	1.67 ±	1.60	1995.8808	2003.4151
SEY1	-4.674	55.479	7.67 ±	0.65	29.12 ±	1.53	0.00 ±	2.32	1995.3795	2002.5767
Transgariep block										
HRAO	-25.890	27.687	15.88 ±	0.41	18.38 ±	0.66	-0.06 ±	0.93	1996.7418	2003.4151
RBAY	-28.796	32.078	14.64 ±	0.73	16.43 ±	0.71	5.70 ±	1.62	2000.8019	2003.4151

Table 2. Plate angular velocity solutions in the NB-SM system

Plate	Reference frame	Plate angular velocity			Source
		Lat	Long.	Rate	
		°N	°E	°/Myr ccw	
NB	**ITRF2000**	**49.9**	**276.2**	**0.258**	**This study**
NB	ITRF97	52.25	279.82	0.253	Sella, Dixon & Mao (2002) [8]
NB	ITRF2000	49.8	278.7	0.258	C DeMets, pers. comm. (2002)
NB	NNR	54.5	273.8	0.280	Kreemer & Holt (2001) [7]
NB(AF)	NNR (3 Ma)	50.65	285.92	0.291	DeMets et al. (1994) [2]
SM	**ITRF2000**	**45.7**	**249.9**	**0.37**	**This study**
SM	ITRF97	53.51	258.45	0.31	Sella, Dixon & Mao (2002) [8]
SM	ITRF2000	51.9	267	0.293	C DeMets, pers. comm. (2002)
SM	NNR	54.6	274.7	0.292	Kreemer & Holt (2001) [7]
NB	**SM**	**-27.06**	**35.94**	**0.148**	**This study**
NB	SM	-35.49	24.02	0.085	Sella, Dixon & Mao (2002) [8]
NB	SM	-41.34	24.75	0.051	C DeMets, pers. comm. (2002)
NB	SM	-31	28	0.04	C Kreemer, pers. comm. (2002)
NB	SM	-54.98	295.93	0.012	Kreemer & Holt (2001) [7]
NB	SM	-27.3	36.2	0.089	Chu & Gordon (1999) [5]

FIGURE CAPTIONS

Fig. 1. GPS sites (*labeled diamond symbols*) around the Nubia (NB) – Somalia (SM) plate boundary in Africa. Stippled lines mark belts of more intense seismicity around smaller Ukerewe Nyanza (UN), Rovuma (RV), Transgariep (TG) and possible Lwandle (LW?) tectonic blocks (after ref. 11). Epicentres (black dot symbols) are from the intracontinental earthquake catalogue of Triep and Sykes [32].

Fig. 2. Times-series plot of North, East and Vertical components of position for the Hartebeesthoek (HRAO) GPS site during the 6.73–year period between 1996.7418 and 2003.4151. The daily data (from server at http://sopac.ucsd.edu/cgi-bin/refinedTimeseriesListing.cgi) is fitted by a refined model (*grey/red line*) that incorporates a linear slope, representing plate-tectonic rotation, and annual and semi-annual periodicities, representing site fluctuations related to hydroclimatic or other transient factors.

Fig. 3. Graphical solution from three sites for the NB plate angular velocity in the ITRF2000 reference frame.

(a) Lower hemisphere, equal angle stereogram centred on South pole, 0°E on equator at top. *Solid black symbols* are southern hemisphere GPS sites: NKLG (*triangle*), SUTH (*square*) and GOUG (*diamond*). *Smaller open symbols* are poles at 90° from GPS sites along longitudinal planes through geocentre. *Larger open symbols* are geocentre-projected positions (antipodes) of the tangential (horizontal) velocity vectors for each site, e.g., the angle between the large and small open squares, measured in the plane normal to the SUTH site vector (*dashed great circle*), is equal to the N42.1° E azimuth of the GPS-measured SUTH velocity vector. The best-fitting plane to the projected velocity vectors (*solid great circle*) is normal to the NB plate angular-velocity pole (*large target symbol* plotted at its southern hemisphere antipode), and contains the maximum (*solid circle*) and intermediate (*open circle*) eigenvectors to the velocity orientation tensor.

(b) Plot of site velocity residuals versus NB-ITRF2000 rotation rate about the NB angular-velocity pole in (a) above.

Fig. 4. Graphical solution from two sites for the SM plate angular velocity in the ITRF2000 reference frame.

(a) Lower hemisphere, equal angle stereogram centred on South pole, 0°E on equator at top. *Solid black symbols* are southern hemisphere GPS sites: MALI (*square*) and SEY1 (*diamond*). Other symbols as in Fig. 3(a).

(b) Plot of site velocity residuals (observed-model) versus SM-ITRF2000 rotation rate about the SM angular-velocity pole in (a) above.

Fig. 5. Velocity vector diagrams for four sites on the NB plate. Measured velocity vectors from Table 1 (*diamond symbol with standard error bars* on *thicker solid line* to origin) are compared with NB-ITRF2000 velocity model from Fig. 3 above (*solid circle on thin solid line*) and NB-ITRF97 velocity model from Sella et al. (2002; *open circle on dashed line*). For site MAS1 (*lower right block*), not used in the present solution, additional comparison is made with the Eurasia (EU)-ITRF96 model from Nocquet et al. (2001).

Fig. 6. Velocity vector diagrams for two sites on the SM plate. Measured velocity vectors from Table 1 (*diamond symbol with standard error bars* on *thicker solid line* to origin) are compared with SM-ITRF2000 velocity model from Fig. 4 above (*solid square on thin solid line*) and SM-ITRF97 velocity model from Sella et al. (2002; *open square on dashed line*).

Fig. 7. Velocity vector diagrams for HRAO and RBAY sites on the Transgariep (TG) block. Measured velocity vectors from Table 1 (*diamond symbol with standard error bars* on *thicker solid line* to origin) are compared with NB- and SM-ITRF2000 velocity models from Figs. 3 & 4 above (respectively *solid square on thin solid, and solid circle on dash-dotted lines*) and NB- and SM-ITRF97 velocity models from Sella et al. (2002; respectively *open square on thin solid, and open circle on dashed lines*).

Fig. 8. NB-SM angular velocity poles (*numbered ring symbols*) in relation to the wide plate boundary zone and GPS sites (*labelled diamond symbols*) in Southern and Eastern Africa. NB rotates anticlockwise relative to SM about the pole location. Recent motion pole (No. 1) from this study overlaps with the NUVEL1A-based (~3 Myr) solution of Chu & Gordon (1999; pole No. 5). Other poles are from Sella et al. (2002, pole No. 2), DeMets (2002, pole No. 3), and Kreemer (2002, pole No. 4). NB-SM poles farther west or south (Table 2) are not shown.

FIGURES

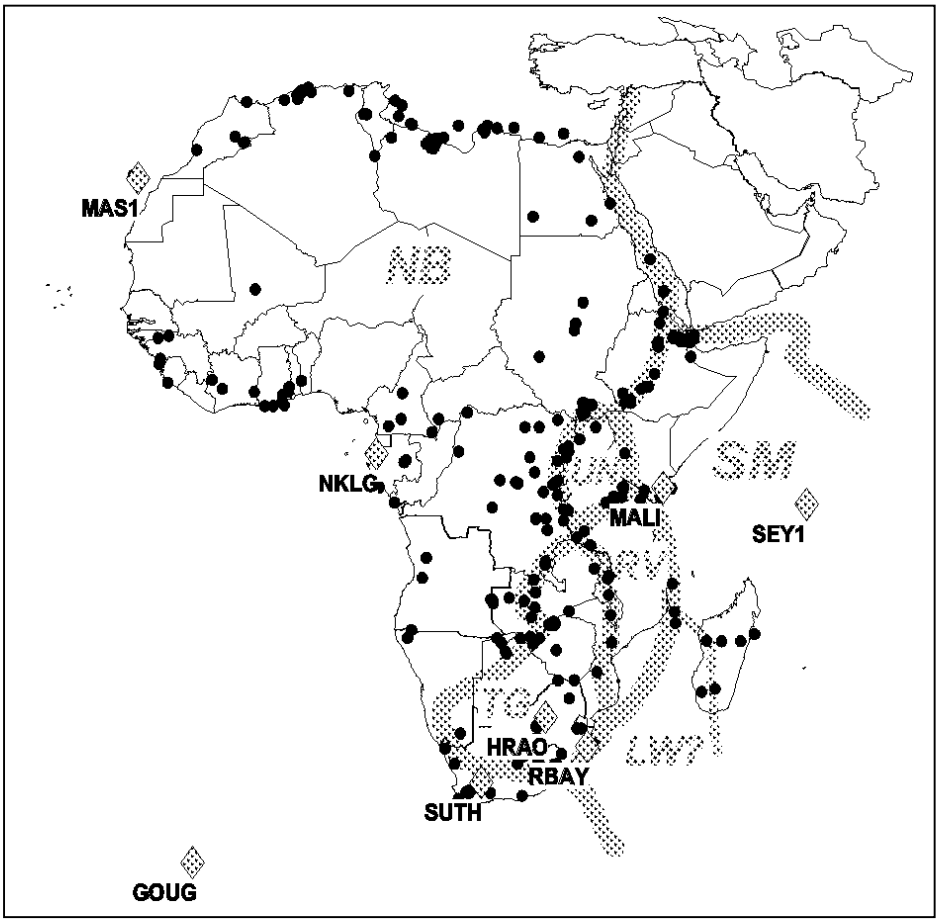

Fig.1

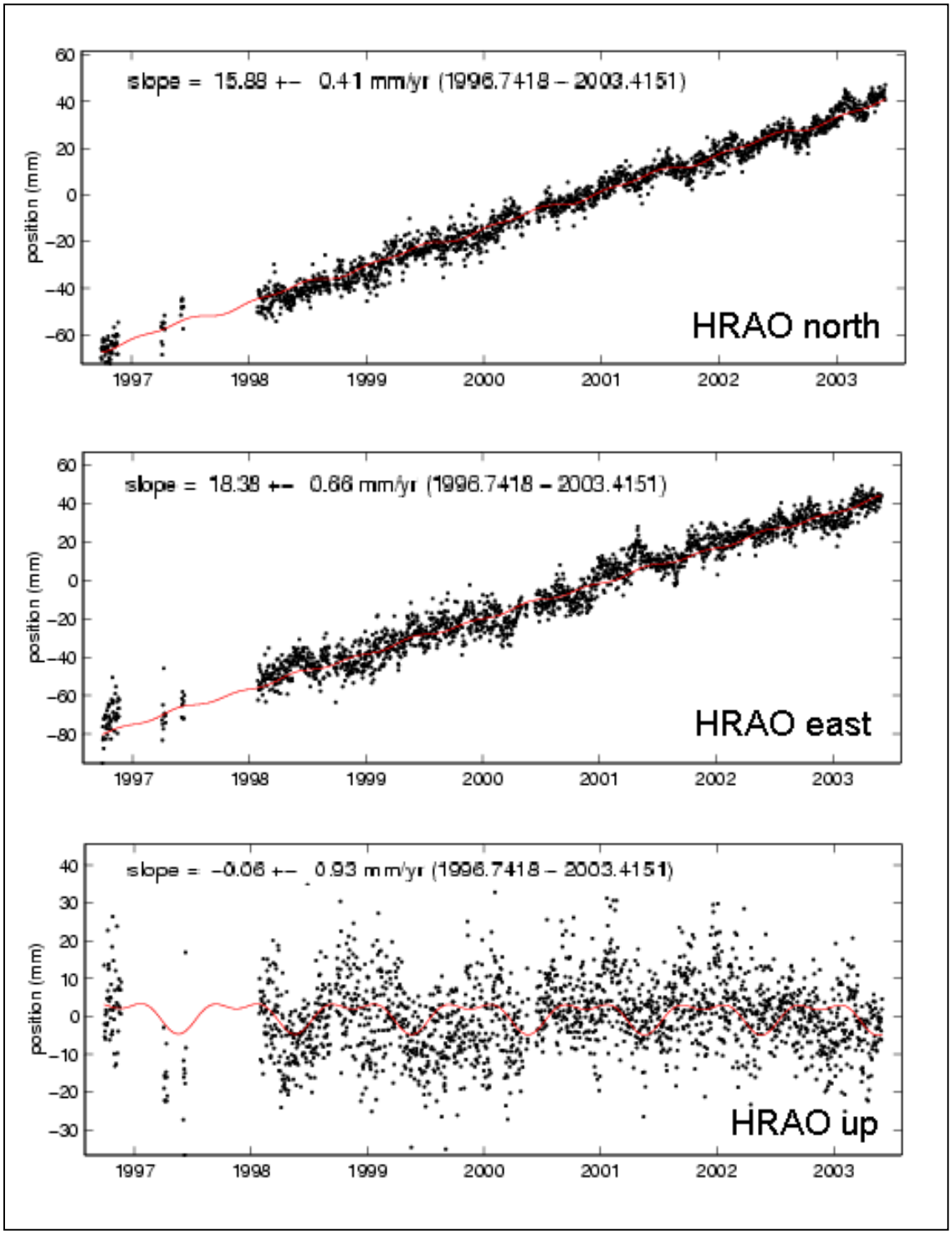
slope = 15.89 +- 0.41 mm/yr (1996.7418 – 2003.4151)
position (mm)
HRAO north
slope = 18.38 +- 0.66 mm/yr (1996.7418 – 2003.4151)
position (mm)
HRAO east
slope = -0.06 +- 0.93 mm/yr (1996.7418 – 2003.4151)
position (mm)
HRAO up
1997
1998
1999
2000
2001
2002
2003

Fig. 2

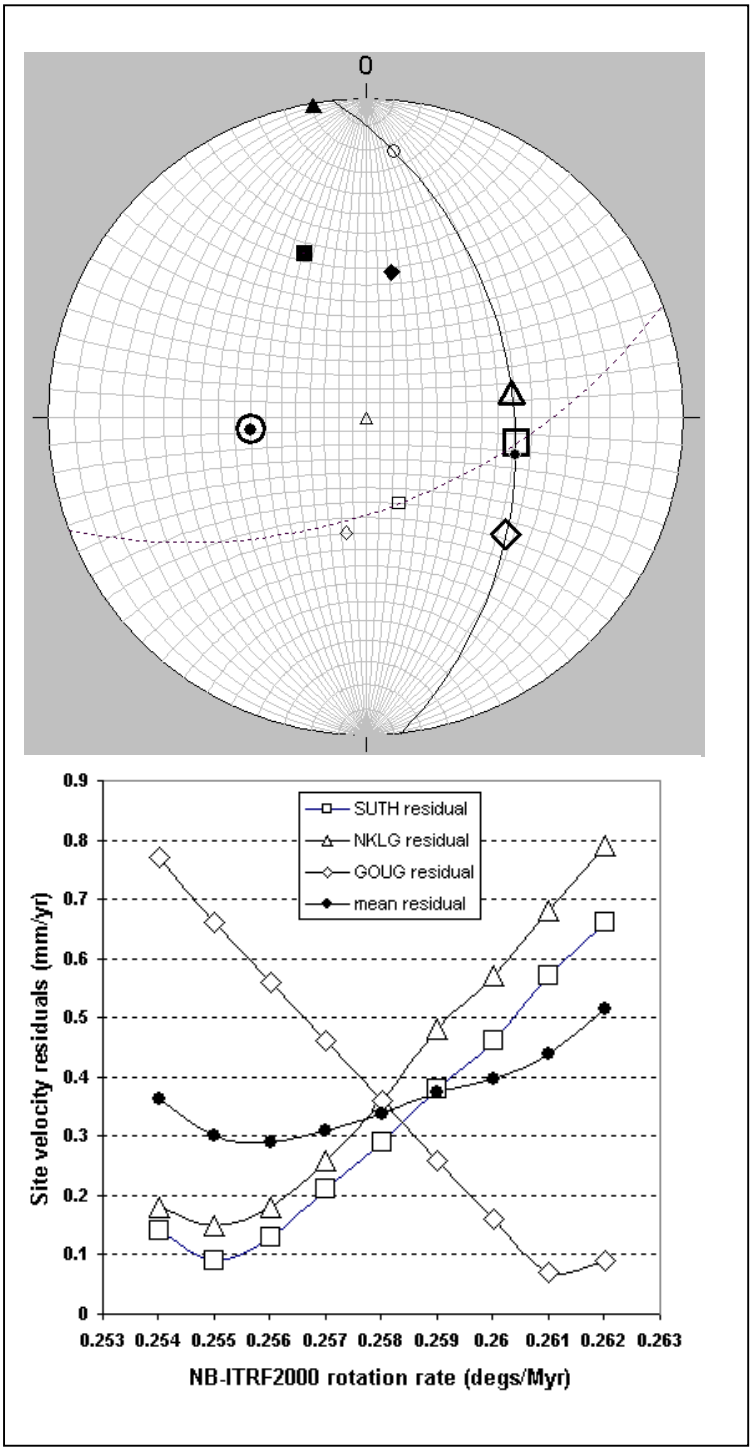
0
SUTH residual
NKLG residual
GOUG residual
mean residual
Site velocity residuals (mm/yr)
0
0.1
0.2
0.3
0.4
0.5
0.6
0.7
0.8
0.9
0.253 0.254 0.255 0.256 0.257 0.258 0.259 0.26 0.261 0.262 0.263
NB-ITRF2000 rotation rate (degs/Myr)

Fig. 3

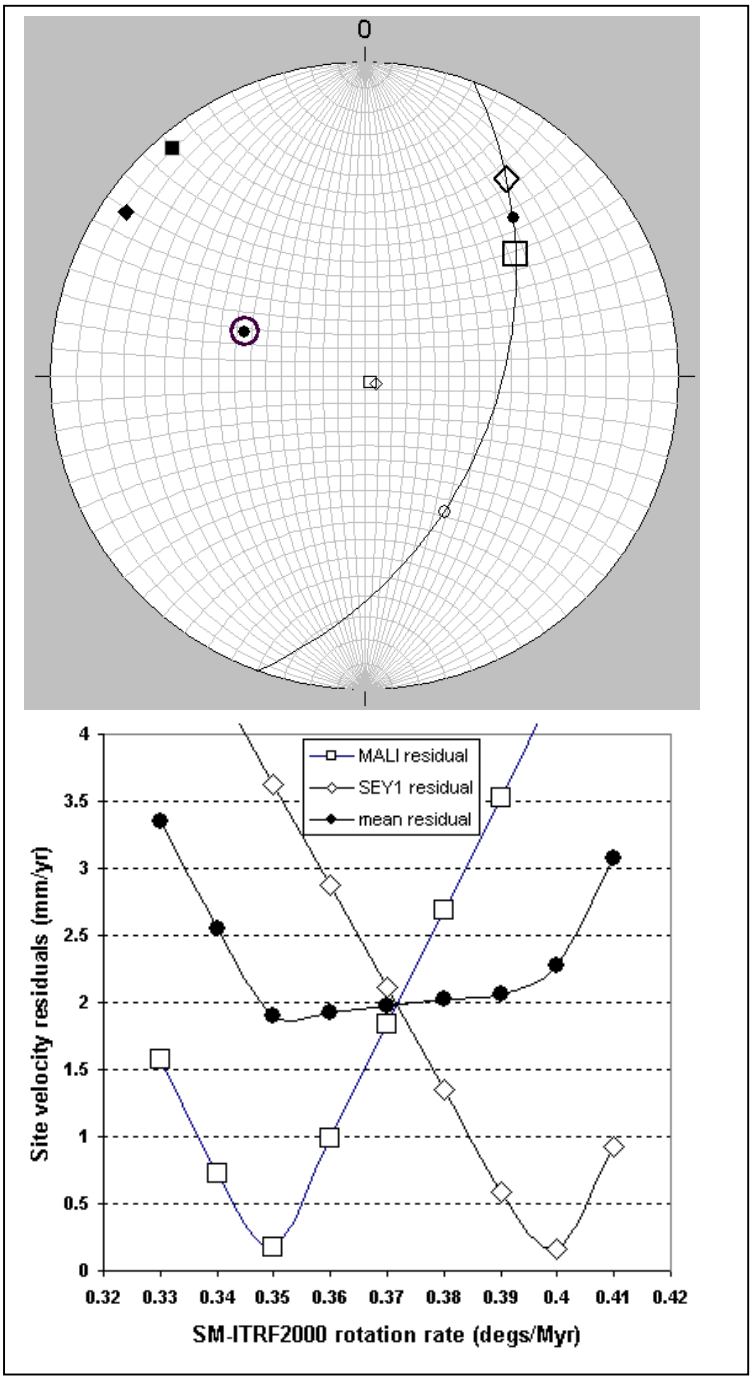
0
MALI residual
SEY1 residual
mean residual
Site velocity residuals (mm/yr)
SM-ITRF2000 rotation rate (degs/Myr)
0
0.5
1
1.5
2
2.5
3
3.5
4
0.32
0.33
0.34
0.35
0.36
0.37
0.38
0.39
0.4
0.41
0.42

Fig. 4

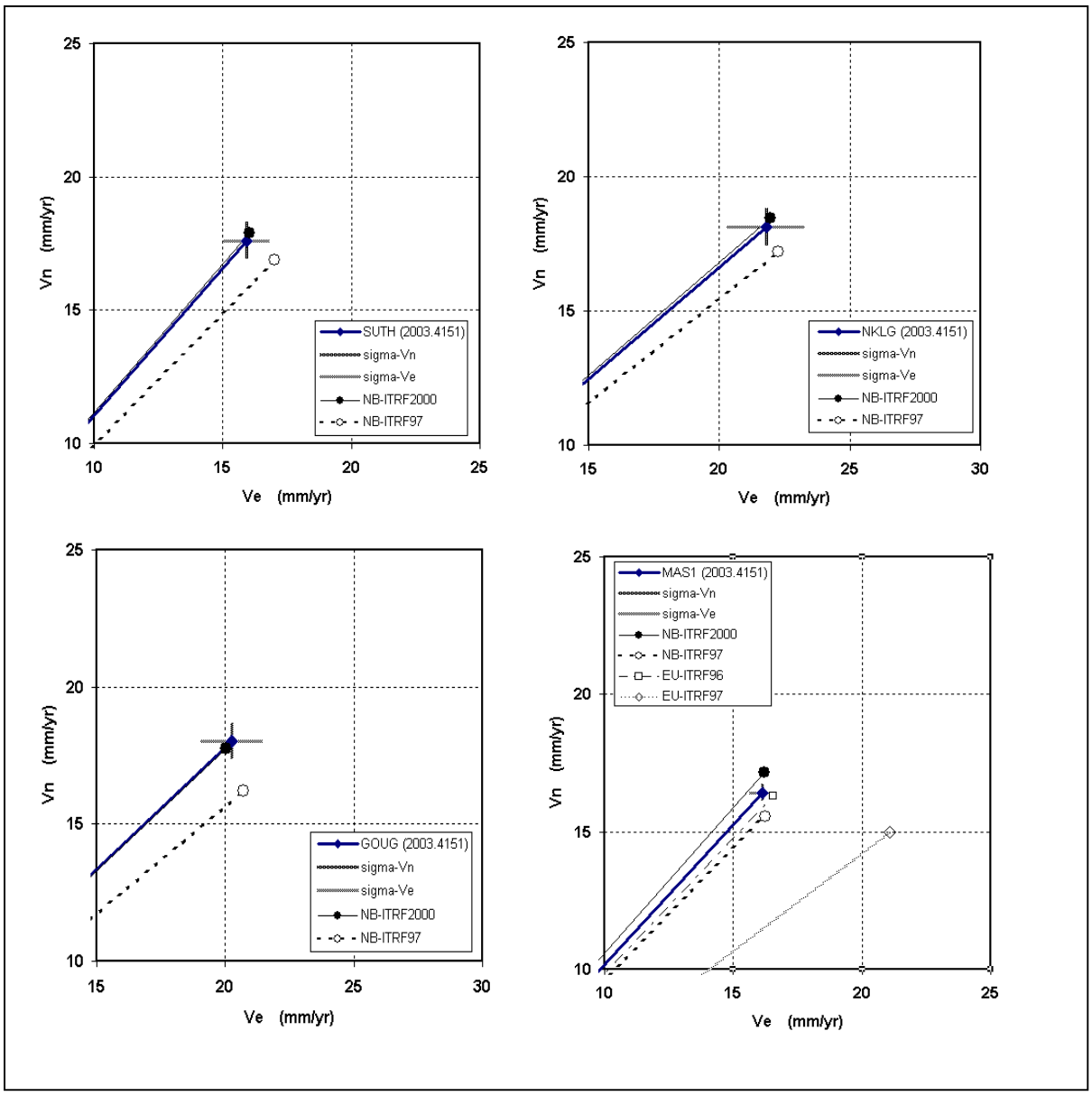
Vn (mm/yr)
Ve (mm/yr)
SUTH (2003.4151)
sigma-Vn
sigma-Ve
NB-ITRF2000
NB-ITRF97
NKLG (2003.4151)
GOUG (2003.4151)
MAS1 (2003.4151)
EU-ITRF96
EU-ITRF97

Fig. 5

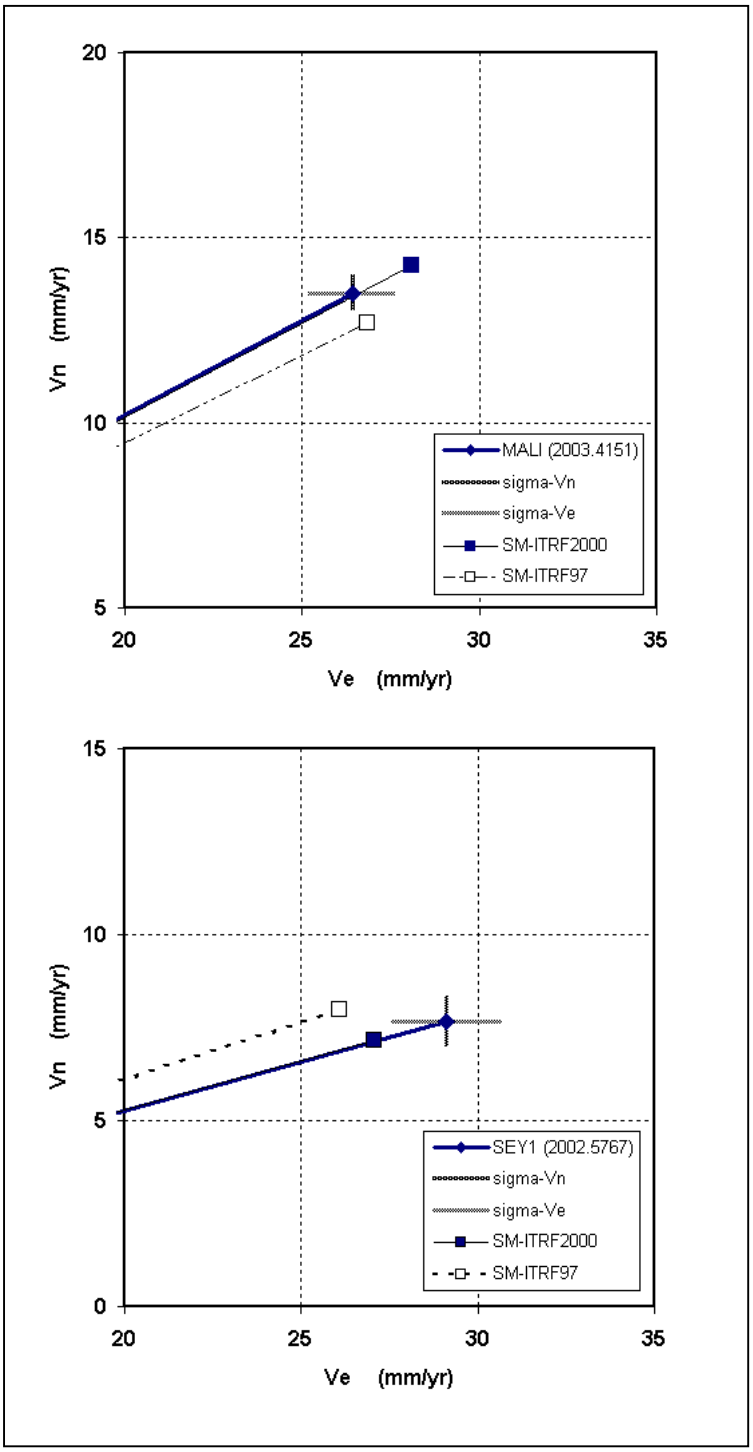
20
15
10
5
Vn (mm/yr)
20
25
30
35
Ve (mm/yr)
MALI (2003.4151)
sigma-Vn
sigma-Ve
SM-ITRF2000
SM-ITRF97
15
10
5
0
Vn (mm/yr)
20
25
30
35
Ve (mm/yr)
SEY1 (2002.5767)
sigma-Vn
sigma-Ve
SM-ITRF2000
SM-ITRF97

Fig. 6

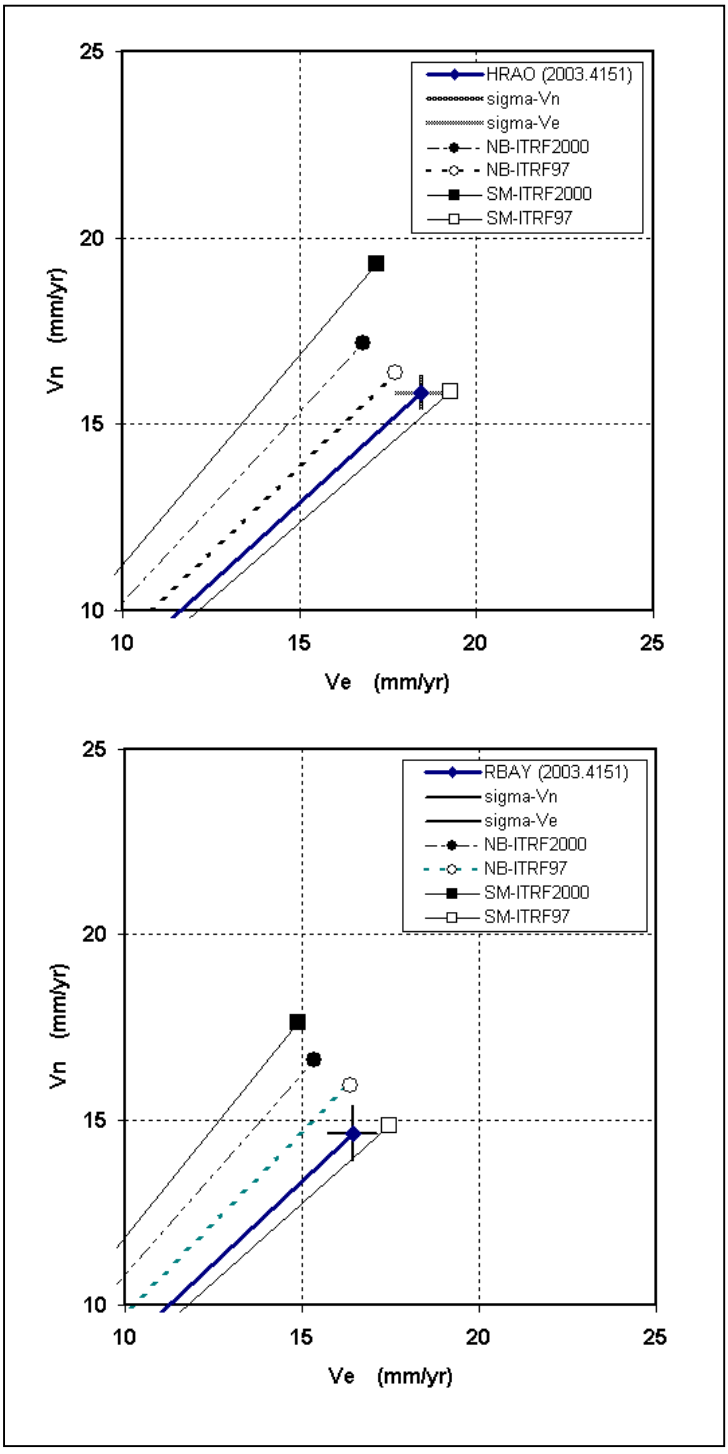
HRAO (2003.4151)
sigma-Vn
sigma-Ve
NB-ITRF2000
NB-ITRF97
SM-ITRF2000
SM-ITRF97
Vn (mm/yr)
Ve (mm/yr)
25
20
15
10
RBAY (2003.4151)
sigma-Vn
sigma-Ve
NB-ITRF2000
NB-ITRF97
SM-ITRF2000
SM-ITRF97
Vn (mm/yr)
Ve (mm/yr)

Fig. 7

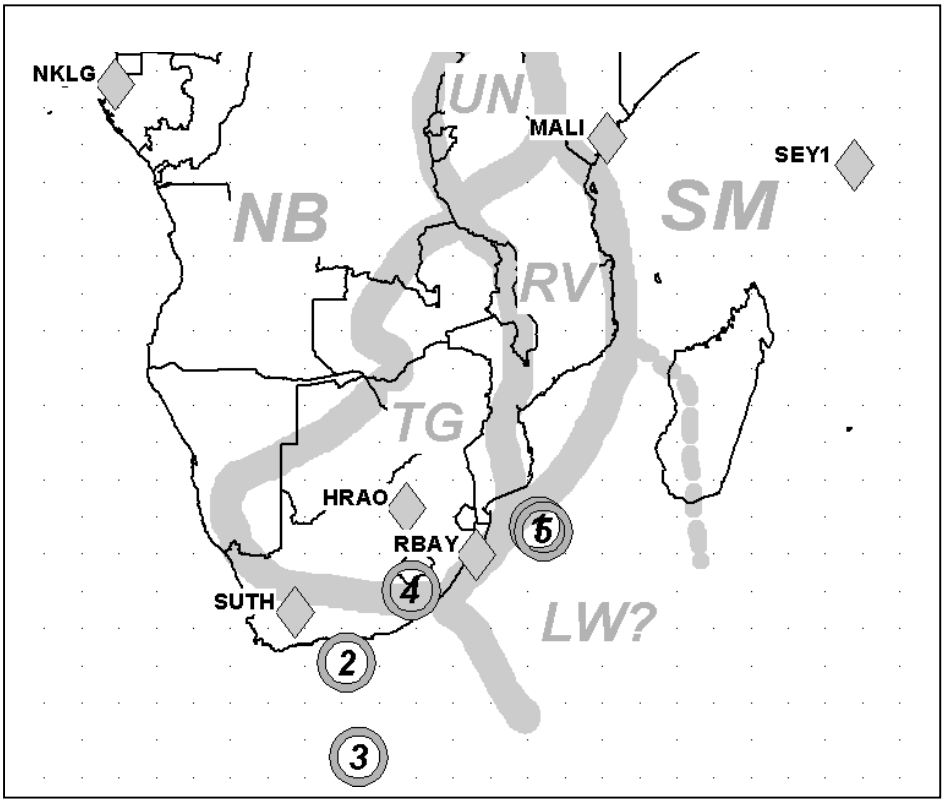

Fig. 8